Int. J. Multiphase Flow Vol. 16, No. 6, pp. 1047–1069, 1990
Printed in Great Britain.

0301-9322/90 $3.00 + 0.00

COMPRESSIBLE FLOW OF A TWO-PHASE FLUID BETWEEN FINITE VESSELS—I

IDEAL CARRIER GAS

D. R. CHENOWETH
Applied Mechanics Department, Sandia National Laboratories, Livermore, CA 94551-0969, U.S.A.

S. PAOLUCCI
Department of Aerospace and Mechanical Engineering, University of Notre Dame, Notre Dame, IN 46556-9956, U.S.A.

(*Received* 30 *March* 1990; *in revised form* 19 *July* 1990)

Abstract—The transfer of a multiphase fluid from a high-pressure vessel to one initially at lower pressure is investigated. The fluid is composed of two phases which do not undergo any change. The phases consist of an ideal gas, and solid particles (or liquid droplets) having constant density. The mixture is assumed to be stagnant and always perfectly mixed as well as at thermal equilibrium in each constant volume vessel. The fluid also remains homogeneous and at equilibrium while flowing between vessels. The transport properties of the mixture are taken to be zero. One important finding is that the expanding mixture or pseudo-fluid behaves similarly to a polytropic Abel–Noble gas. The mixture thermodynamic properties, the end state in each vessel at pressure equilibrium, the critical parameters and time-dependent results are given for the adiabatic and isothermal limiting cases. The results include both initially sonic and initially subsonic transfers. No mathematical restriction is placed on the particle concentration, although some limiting results are given for small particle volume fraction. The mass transferred at adiabatic pressure equilibrium can be significantly less than that when thermal equilibrium is also reached. Furthermore, the adiabatic pressure equilibrium level may not be the same as that obtained at thermal equilibrium, even when all initial temperatures are the same. Finally, it is shown that the transfer times can be very slow compared to those of a pure gas due to the large reduction possible in the mixture sound speed.

Key Words: homogeneous, equilibrium, two-phase, ideal gas, finite volume, compressible, transfer

1. INTRODUCTION

The rapid transfer of both ideal and non-ideal gas, between finite volume reservoirs connected in a variety of ways, has been studied extensively by Chenoweth (1974, 1979, 1983). Many physical effects can independently alter the behavior in such problems. In order to understand how each parameter enters the problem, and which ones are dominant for particular cases, great care must be exercised in the analysis. The use of limiting analyses helps bound the results, and prevents attributing peculiar behaviors to the wrong physical causes. This is even more important when the transfer involves a multiphase fluid, because the additional parameters which enter the problem can have first order effects which are not always expected or easy to explain. The effect of the mixture equation of state and the corresponding sound speed behavior are examples of this sort of phenomenon.

Only homogeneous equilibrium two-phase mixtures are investigated here. It is shown that such a mixture, where the carrier gas is behaving as an Abel–Noble gas (non-ideal effects are described by the first term of a co-volume virial expansion in pressure), also behaves as an Abel–Noble fluid. The mixture co-volume depends linearly on the constant particle mass fraction to combine the gas and particle effects. This Abel–Noble fluid has a modified gas constant and undergoes a polytropic expansion from the supply because the adiabatic index (mixture ratio of specific heats) is then constant and lies between the isothermal limit of unity and the gas ratio of specific heats. The transfer of a pure Abel–Noble gas is well-understood (Chenoweth 1983). Although we present detailed results only for an ideal carrier gas, the Abel–Noble fluid mixture does have some features in common with similar pure gas results.

The mixture sound speed can have a very complicated behavior, compared to the relatively simple Abel–Noble gas case, even when the carrier gas is ideal (the gas density is negligible compared to the gas co-density constant). It can, in fact, have values much smaller than the gas sound speed for many combinations of the parameters. Some aspects of this physical phenomenon were originally discussed by Sewell (1910). For transfer problems controlled by an orifice or nozzle between the reservoirs (rather than a long pipe) the supply sound speed is the dominant fluid property. Thus, the importance of fully understanding its effect is paramount to the transient study of two-phase fluid transfer. The final state, of course, is determined from the equation of state without ever considering the sound speed.

A wide variety of expressions for sound speed have been derived for different limiting conditions. Marble (1970) discusses several limits and gives different expressions, all valid for small particle volume fractions applicable to dusty-gas. Schmitt-von Schubert (1969) gives analogous expressions without restrictions on volume fraction. For the case of gas bubbles within a liquid carrier, Wood (1941, 1955), Karplus (1958), Wallis (1969), Henry & Grolmes (1971) and van Wijngaarden (1972) give expressions for arbitrary gas volume fraction in the isothermal limit, as well as more restricted expressions valid in other limits which they discuss. Henry & Grolmes (1971) give generalized expressions also valid for phase change and discuss the limitations of the various approximations, along with data comparisons, in perhaps the greatest detail of any of the references given here. Recent papers by Gumerov *et al.* (1988), and Ruggles *et al.* (1988) review and summarize much of the past work and examine the role of the excitation frequency in the transition from equilibrium to the frozen limit. Apparently, Ackeret (1930) originally derived some of these limiting expressions for application to gas–water mixtures, while others first appear in Wood (1941). Heinrich (1942) gives the equilibrium sound speed for a homogeneous mixture undergoing an isentropic expansion, and discusses some of its characteristics. Tangren *et al.* (1949) rederive the same expressions and apply them to de Laval nozzle flow. Additionally, they obtain critical property ratios in the isothermal limit and present tables for the parameter range applicable to homogeneous water–gas mixture flow. They give limited experimental evidence to support the nozzle flow analysis using the critical properties derived there. A major finding of Henry & Grolmes (1971), which seems to be supported by the data of Ruggles *et al.* (1988), is that a small pressure pulse travels at much higher velocity and with stronger dependence on volume fraction, compared to the highly frequency-dependent sound speed. This finding must be considered when sound speed experiments are tested for validity using existing data.

Most of the existing experimental data on sound speed is for air–water and vapor–water mixtures (Karplus 1958, 1961; Semenov & Kosterin 1964; Silberman 1957), and the existence of minimum values much less than those of the gas has been demonstrated in these cases. Known expressions adequately predict the large changes in sound speed over a wide range of volume fractions. Additionally, Nguyen *et al.* (1981) compare several *ad hoc* sound speed equations to the above data and obtain reasonable agreement in most cases, particularly near the minimum. Some experimental data that we are aware of which deals with solid–particle/gas mixtures are those of Zink & Delsasso (1958), Soo (1960) and Guenoche *et al.* (1988). Zink & Delsasso (1958) only investigate dilute volume concentrations of Al_2O_3 (alumina) in a variety of carrier gases, thus their results have limited usefulness in verifying the sound speed variation over a wide range of volume fractions. Similarly, Soo (1960) gives data for small volume fractions of magnesia carried by air. Guenoche *et al.* (1988) use steel and glass spheres in nitrogen with volume fractions ranging from 0.595 to 0.66, resulting in a fixed bed configuration. Since this high volume fraction study obtains the sound speed by measuring the velocity of the head of an unsteady rarefaction wave, it is not clear that the sound speed is actually reported there, since the data of Henry & Grolmes (1971) and Ruggles *et al.* (1988) show that a large difference exists between the speeds of a pressure pulse and that of sound, at least for vapor–water mixtures.

In this work, the equilibrium isentropic sound speed expression is applied to the transfer of a homogeneous gas–particle mixture between two finite vessels joined by a nozzle or an orifice to control the flow. Thus, there are zero spacial dimensions and negligible volume between the stagnant reservoirs. In addition, the transfer is quasi-steady in the sense that the steady, integrated Euler equation is applied across the flow control region at each instant of time, as in pure gas analyses. The effects of non-isothermal flow on the critical properties, the supply and receiving

vessel end states, as well as the transfer time to pressure equilibrium are investigated for a wide range of parameters. Analytical limiting solutions are given for some special parameter values, but generally the governing equations must be solved numerically. No attempt is made here to include the many other flow regimes which are possible [see Henry & Grolmes (1971) or Wallis (1969)] or to define the physical limitations of the model used; these difficult tasks are clearly beyond the scope of the current paper.

2. MIXTURE THERMODYNAMIC PROPERTIES

The mixture thermodynamic properties, analogous to those given by Heinrich (1942) and Tangren *et al.* (1949), are given in this section to establish nomenclature and form the foundation for the following sections. Furthermore, many of the properties are extended in several areas to better clarify the nature of the mixture behavior.

2.1. Equation of State

The mixture density ρ can be written as

$$\rho = \left[\frac{1-\phi}{\rho_G} + \frac{\phi}{\rho_d}\right]^{-1} = (1-\theta)\rho_G + \theta\rho_d \qquad [1]$$

in terms of the particle mass fraction ϕ or the particle volume fraction θ. Note that $\theta = \phi\rho/\rho_d$. The particle density ρ_d is taken to be constant, and the gas density ρ_G is initially taken to be non-ideal

$$P_G = Z_G \rho_G R_G T_G, \qquad [2]$$

where the pressure P, the temperature T, the compressibility factor Z and the gas constant R are identified in the gas phase by the subscript G. Since

$$\rho_G = \rho \frac{1-\phi}{1-\theta}, \qquad [3]$$

then for $P = P_G$ (no particle contribution to pressure) and $T = T_d = T_G$ (no thermal lag), the mixture equation of state can be written as

$$P = Z\rho RT. \qquad [4]$$

The above equation of state is written in terms of a mixture gas constant

$$R = (1-\phi)R_G, \qquad [5]$$

and "compressibility" factor

$$Z = \left(1 - \frac{\rho}{d}\right)^{-1} = \frac{Z_G}{1-\theta}, \qquad [6]$$

where

$$d = \left[\frac{1-\phi}{d_G} + \frac{\phi}{d_d}\right]^{-1}, \qquad [7]$$

provided the gas compressibility factor is given by the Abel–Noble expression (van der Waals gas with negligible intermolecular force term)

$$Z_G = \left(1 - \frac{\rho_G}{d_G}\right)^{-1}, \qquad [8]$$

which is valid when $T \gg T_c$ (T_c is the critical gas temperature). The co-densities d_G and d for the gas and the mixture, respectively, are the inverse of the usual co-volumes and the particle co-density d_d is identified to be ρ_d. Obviously, the mixture described by [6] and [7] also behaves as an Abel–Noble fluid if θ is not negligible compared to unity. In the following work it is assumed that $\rho_G \ll d_G$, so that an ideal carrier gas results ($Z_G = 1$). It should be noted that d_G should be

determined from PVT data (Chenoweth 1983), since it cannot be reliably obtained from critical property information. The effects of $Z_G \neq 1$ will be examined in part II (Chenoweth & Paolucci 1990b) where an Abel–Noble carrier gas is used.

2.2. Specific Heat Ratio

The mixture specific heat ratio $\gamma = C_P/C_V$ can be written in terms of the particle mass fraction, the gas specific heat ratio $\gamma_G = C_{P_G}/C_{V_G}$ and $\delta = C/C_{P_G}$, where C is the particle heat capacity:

$$\gamma = \gamma_G\left[\frac{1-\phi(1-\delta)}{1-\phi(1-\delta\gamma_G)}\right]; \qquad [9]$$

using the mixture specific heats at constant pressure and volume,

$$C_P = \phi C + (1-\phi)C_{P_G} \qquad [10]$$

and

$$C_V = \phi C + (1-\phi)C_{V_G}, \qquad [11]$$

where C and the gas heat capacities are taken to be independent of T (calorically perfect gas). The behavior of the mixture specific heat ratio is shown in figure 1; note that $1 \leqslant \gamma \leqslant \gamma_G$. When $\delta \ll 1$ or $\phi\delta \ll 1$, $\gamma \to \gamma_G$ results, while the isothermal limit $\gamma \to 1$ is obtained when $\gamma_G \to 1$, $\phi \to 1$ or $\phi\delta \gg 1$. It must be emphasized that ϕ, and therefore γ, are constants in the expansion region upstream of the minimum flow area, directly as a result of the previous assumptions. Obviously, if the initial receiver mass fraction is different from that in the supply, then the receiver mass fraction will not be constant during the transfer.

2.3. Isentropic Relations

In a reversible adiabatic expansion with constant particle mass fraction (no relative velocity between gas and particles) Heinrich (1942) and Tangren *et al.* (1949) obtain the following relations:

$$T\rho_G^{-(\gamma-1)} = C_1, \qquad [12]$$

$$P\rho_G^{-\gamma} = C_2 \qquad [13]$$

and

$$PT^{-\gamma/(\gamma-1)} = C_3, \qquad [14]$$

where C_1, C_2 and C_3 are constants. Only the presence of γ instead of γ_G alters these relations from the well-known ideal gas expressions. Since γ is constant when ϕ is constant, then γ corresponds to a true polytropic exponent which is bounded by unity and γ_G.

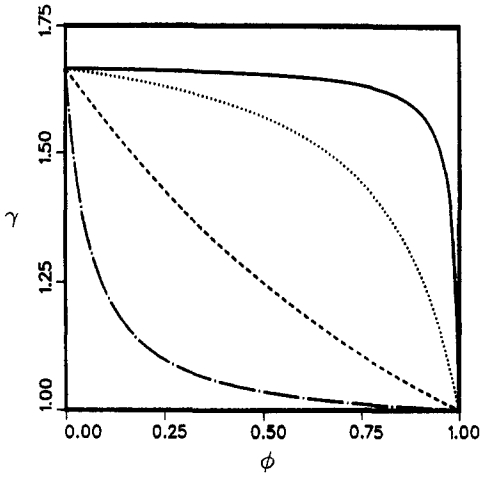

Figure 1. Mixture ratio of specific heats vs particle mass fraction for $\gamma_G = 5/3$ with δ as the parameter: ——, $\delta = 10^{-2}$; ·····, $\delta = 10^{-1}$; – – – –, $\delta = 1$; — · — ·, $\delta = 10$.

2.4. *Adiabatic Sound Speed*

When [1] is differentiated with respect to P (with ϕ constant) we obtain

$$\frac{d\rho}{dP} = \left[\frac{(1-\theta)^2}{(1-\phi)}\frac{d\rho_G}{dP} + \frac{\theta^2}{\phi}\frac{d\rho_d}{dP}\right]. \quad [15]$$

Often $dP/d\rho_G$ and $dP/d\rho_d$ are identified or interpreted as pseudo-isothermal gas and particle sound speeds squared, respectively, and $dP/d\rho$ is the corresponding mixture value. This interpretation is only valid for very slow processes which involve low frequencies. More generally, for rapid expansions the derivatives in [15] should be evaluated at constant entropy. Using [13], we get

$$\frac{d\rho_G}{dP} = \frac{\rho_G}{\gamma P} = \frac{\gamma_G}{\gamma a_G^2}, \quad [16]$$

in terms of the adiabatic gas sound speed a_G. It is obvious that the "isothermal" and "adiabatic" limits of Wallis (1969) are recovered from [16] when $\gamma \to 1$ and $\gamma \to \gamma_G$, respectively. In this work, the last term in [15] vanishes since ρ_d is constant. In the more realistic case where ρ_d is not constant, the necessary approximation to neglect the last term is

$$\frac{dP}{d\rho_d} \gg \left(\frac{\gamma}{\gamma_G}\right)\left(\frac{\theta}{1-\theta}\right)^2\left(\frac{1-\phi}{\phi}\right)a_G^2. \quad [17]$$

The mixture sound speed $a = \sqrt{dP/d\rho}$ can then be written as

$$a = \frac{a_G}{(1-\theta)}\left[\frac{\gamma}{\gamma_G}(1-\phi)\right]^{\frac{1}{2}}, \quad [18]$$

where

$$a_G = (\gamma_G R_G T_G)^{\frac{1}{2}}. \quad [19]$$

This adiabatic equilibrium sound speed represents the low frequency limit (Gumerov *et al.* 1988). The high frequency (frozen) limit results in $a \to a_G$ and is not included in the analysis below. Note that the mixture adiabatic sound speed only changes in an expansion due to the dependence on θ and a_G (via T), since ϕ and γ remain fixed. However, since the initial supply sound speed controls the transfer time scale (Chenoweth 1974, 1983), it is important to understand how [18] is affected by all parameters. For the purpose of examining the behavior of [18], the density ratio

$$r = \frac{\rho_G}{\rho_d} = \left(\frac{1-\phi}{\phi}\right)\left(\frac{\theta}{1-\theta}\right) \quad [20]$$

is introduced; then [18] becomes

$$\left(\frac{a}{a_G}\right)^2 = \frac{r[r-\theta(r-\delta)]}{(1-\theta)[r-\theta(r-1)][r-\theta(r-\delta\gamma_G)]}. \quad [21]$$

The pure gas and solid limits are recovered since if $\theta \to 0$, $a \to a_G$, while for $\theta \to 1$, $a \to \infty$. It can be shown that $a_G < a < \infty$ only when $r > [1+\delta(\gamma_G - 1)]/2$. However, for constant r in the range $0 \leqslant r < [1+\delta(\gamma_G-1)]/2$, a minimum sound speed exists such that $a_{min} < a_G$ in the physical region $0 \leqslant \theta \leqslant 1$. This behavior is illustrated in figure 2 where a/a_G is plotted vs θ with r as a parameter for $\gamma_G = 5/3$, $\delta = 0.01$ and $\delta = 1$. It appears that there is often a wide range of θ values near 1/2 having sound speed close to the minimum, so this value is quite useful to know. For some purposes, when the volume fraction remains in this range, the sound speed can be taken to be independent of θ and assumed to be at its minimum level.

The explicit value of volume fraction at which the minimum sound speed occurs is given by

$$c_3\theta^3 + c_2\theta^2 + c_1\theta + c_0 = 0, \quad [22]$$

where the coefficients c_0, c_1, c_2 and c_3 are functions of r, δ and γ_G. These coefficients are given explicitly by Chenoweth & Paolucci (1990a) where useful limiting solutions are also given for five special cases identified by $\delta = 1$, $r \ll \delta$, $r = 1$, $r = \delta$ and $r = \delta\gamma_G$, as well the criterion for selecting the physically correct general solution from the three real roots of [22]. This solution is substituted

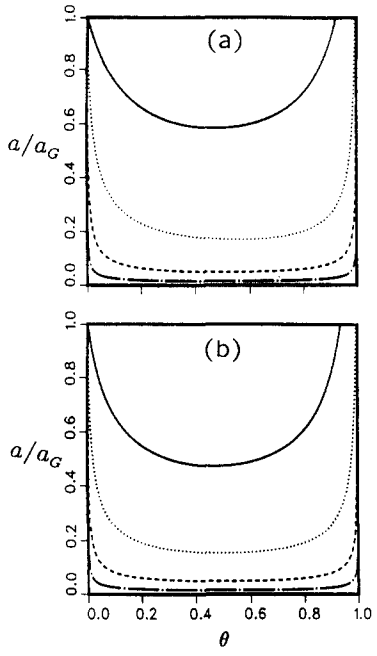

Figure 2. Mixture sound speed vs particle volume fraction for $\gamma_G = 5/3$ with r as the parameter. (a) $\delta = 10^{-2}$, (b) $\delta = 1$: ——, $r = 10^{-1}$; ·····, $r = 10^{-2}$; – – – –, $r = 10^{-3}$; — · — ·, $r = 10^{-4}$.

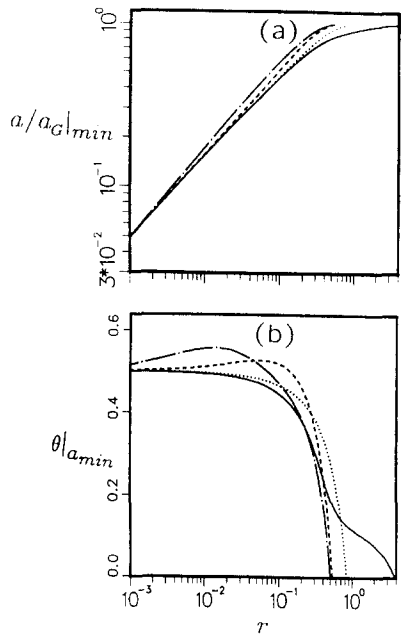

Figure 3. (a) Minimum sound speed and (b) corresponding particle volume fraction vs r for $\gamma_G = 5/3$ with δ as the parameter: ——, $\delta = 10$; ·····, $\delta = 1$; – – – –, $\delta = 10^{-1}$; — · — ·, $\delta = 10^{-2}$.

into [21] to find the minimum of $(a/a_G)^2$ at that volume fraction. Figures 3(a, b) give results for that minimum and its location vs r for various values of δ and $\gamma_G = 5/3$. Although when $r \ll \delta$, $(a/a_G)^2_{min} \to 4r/\gamma_G$ and its location $\theta \to 1/2$, significantly different behavior is obtained for larger values of r.

As an illustration of this behavior, the experimental data of Karplus (1958) for the air–water system (actually for air bubbles carried by water with the aid of a detergent additive) with $0.33 \leqslant \theta \leqslant 0.99$ shows that for low frequencies ($\leqslant 10^3$ Hz), $a_{min} \simeq 20$ m/s near $\theta \simeq 0.5$, at atmospheric conditions compared to $a = 1500$ m/s when $\theta = 1$. Thus, we calculate for 1 atm and 300 K, $a_G = 347.2$ m/s, $\gamma_G = 7/5$, $\delta = 4.158$ and $r = 1.188 \times 10^{-3}$. For these parameter values $r \ll \delta$ and $a_{min} = 2a_G\sqrt{r/\gamma_G} = 20.23$ m/s at $\theta = 0.5000$. Furthermore, $\phi = 0.9988$ and $\gamma = 1.00008$, implying that the isothermal limit holds for these conditions. This conclusion was also reached by Karplus (1958) as well as Wallis (1969) in his analysis of Karplus' data, which shows excellent agreement with the simplified form of [21] for small r over the entire range $0.33 \leqslant \theta \leqslant 0.99$, except of course from [21] $a \to \infty$ as $\theta \to 1$.

As an aside, it should be noted that the air–water and very similar vapor–water data of Henry & Grolmes (1971) and Ruggles *et al.* (1988) for "pressure pulse propagation velocity" show minimum speeds about twice as large as the values just given for sound speed under similar conditions, illustrating the large difference between these two speeds. The pulse propagation velocity depends strongly on volume fraction, whereas sound speed shows strong dependence on the sound wave frequency if it is high enough for non-equilibrium effects to occur. Both two-fluid and relaxation analyses show this strong, but somewhat different, dependence on frequency when departures from equilibrium exist. Temkin & Dobbins (1966a, b) give theoretical (relaxation) derivations and experimental verifications, using oleic acid/nitrogen, which in their simplest forms, for $r \ll 1$, $\theta \ll 1$, and neglecting the often weaker dependence on thermal relaxation, show the sound frequency must be less than $\nu_G \rho_G / \rho_d D_d^2$ in order that the equilibrium expression [18] be valid, and for essentially no frequency dependence to exist. Here ν_G and D_d are the carrier fluid kinematic viscosity and particle (or bubble or droplet) diameter, respectively. Of course for bubble flows $\rho_G \nu_G$ is the liquid carrier dynamic viscosity and ρ_d becomes the bubble density. Clearly, for the same D_d, [18] is valid for much larger sound frequencies with bubble flow than with particles or droplets carried by a gas. Conversely, for the same sound frequency, much larger bubble diameters are

allowed compared to droplet or particle diameters. Nevertheless, it is clear that very fine dispersions of particulate matter of any type greatly increases this frequency limit. Temkin & Dobbins (1966b), Cole & Dobbins (1970), Davidson (1975) and Gumerov *et al.* (1988) all show that the sound frequency must be much smaller than both the dynamic as well as the thermal relaxation time inverses in order for the dilute equilibrium sound speed expression to apply. This means that if the product of 3/2 times the carrier fluid Prandtl number and the ratio of the dispersed phase heat capacity to that of the carrier fluid is greater than unity, then the thermal relaxation dependence becomes dominant. In that case, the dynamic relaxation frequency limitation given above must be scaled by the inverse of this product so that the resulting more restrictive thermal relaxation frequency limitation is obtained. Steen (1986) actually uses a sound speed expression identical to that of Temkin & Dobbins (1966b) with combined thermal and dynamic relaxation time frequency dependence to devise an acoustic method of measuring particle mass fractions of small volume fraction mixtures in gases. It should be noted that the refined relaxation theory of Davidson (1975) and also the two-fluid theory of Ardron & Duffey (1978) seem to indicate that the frequency limitations just discussed may have to be reduced further, by a factor of 5, in order for the equilibrium frequency independent limit to be closely approached. It is not clear what the limitations are on sound frequency and particle size for non-dilute mixtures. It is obvious, however, that $\theta \to 1/2$ results in strong interactions between phases and since neither phase is likely to be dispersed to a great extent in the other, one would expect this region to present the most severe test of any sound speed model.

3. END-STATE RESULTS

Considerable information can be obtained without solving the time-dependent problem by examining the asymptotic end-states at pressure equilibrium under adiabatic and isothermal conditions in terms of the initial data. The importance of such results is relevant to rapid mass transfer since then a quasi-static pressure equilibrium occurs while significant expansive cooling and compressive heating effects still exist in the supply and receiver, respectively. Complete thermal equilibrium of the system is usually approached at a much slower rate than that for pressure, and it is often not allowed to occur due to transfer time constraints. In some cases, a significant amount of mass is transferred following the initial pressure equilibrium, by the ensuing heat transfer, during the approach to the final state. Furthermore, even though the vessel pressures remain approximately equal during this final approach, they may change together significantly while thermal equilibrium is being reached (see the appendix). The maximum possible effects which can occur, can be estimated without considering any details of the convective heat transfer processes. This can be done by comparing the conditions existing at adiabatic pressure equilibrium with those existing at the final end-state. Such a comparison is formulated below using the following normalization by initial supply quantities:

$$\bar{f}_j = \frac{f_j}{f_1(0)}, \qquad [23]$$

where f is any dependent variable, and the subscript j is 1 or 2 denoting supply and receiver, respectively.

3.1. Thermal Equilibrium

The final state, where $t \to \infty$ and both pressure and thermal equilibrium exist, is very easy to obtain since the final gas density is known in terms of the constant total gas mass and volume in the system. Thus, from [2] we have:

$$\bar{P}(\infty) = \bar{T}(\infty)\left(\frac{1+\rho' V'}{1+V'}\right), \qquad [24]$$

where the final system temperature $\bar{T}(\infty)$ is known and it is not necessarily equal to $\bar{T}_2(0)$;

$$V' = \frac{V_{G2}(0)}{V_{G1}(0)} = \bar{V}_2\left[\frac{1-\theta_2(0)}{1-\theta_1(0)}\right], \qquad [25]$$

using the normalized receiver volume $\bar{V}_2 = V_2/V_1$; and

$$\rho' = \frac{\rho_{G2}(0)}{\rho_{G1}(0)} = \frac{\bar{P}_2(0)}{\bar{T}_2(0)}. \quad [26]$$

Similarly, using [2] and [20], the final supply volume fraction is

$$\bar{\theta}_1(\infty) = \left\{\theta_1(0) + [1 - \theta_1(0)]\frac{\bar{T}(\infty)}{\bar{P}(\infty)}\right\}^{-1}. \quad [27]$$

Notice that $\bar{\theta}_2(\infty)$ is obtained from $\bar{\theta}_1(\infty)$ using [30] below, if $\bar{V}_2 \neq 0$.

3.2. *Adiabatic System*

In this section results are expressed in terms of the normalized supply particle volume fraction $\bar{\theta}_1$. The supply expansion is assumed to be isentropic, so that the pressure and temperature can be written as

$$\bar{P}_1 = \bar{\theta}_1^{\gamma_1}\left[\frac{1 - \theta_1(0)}{1 - \bar{\theta}_1\theta_1(0)}\right]^{\gamma_1} \quad [28]$$

and

$$\bar{T}_1 = \bar{P}_1^{1-1/\gamma_1}. \quad [29]$$

Since the supply and receiver volumes as well as the total mass are constant, the receiver particle volume fraction and mass fraction can be written as

$$\bar{\theta}_2 = \bar{\theta}_2(0) + \frac{1 - \bar{\theta}_1}{\bar{V}_2} \quad [30]$$

and

$$\bar{\phi}_2 = \left[\frac{1 - \bar{\theta}_1 + \bar{V}_2\bar{\theta}_2(0)}{1 - \bar{\theta}_1 + \bar{V}_2\bar{\rho}_2(0)}\right]. \quad [31]$$

Here the definition $\bar{\rho}_2(0) = \bar{\theta}_2(0)/\bar{\phi}_2(0)$ requires special attention, as discussed below. When the system is adiabatic, its total internal energy remains constant, and it is independent of the external temperature. The receiver temperature is then obtained from the condition $\bar{E} = \bar{E}_1 + \bar{E}_2$ and the mixture specific heat [11] so that

$$\bar{T}_2 = \left(\frac{\bar{E} - \bar{\theta}_1\bar{T}_1}{1 - \bar{\theta}_1 + \bar{V}_2\bar{\rho}_2(0)}\right)\left(\frac{1 + \phi_1 F_1}{1 + \phi_1\bar{\phi}_2 F_1}\right), \quad [32]$$

where the system energy $\bar{E}$ is given by

$$\bar{E} = 1 + \bar{V}_2\bar{T}_2(0)\bar{\rho}_2(0)\left[\frac{1 + \phi_1\bar{\phi}_2(0)F_1}{1 + \phi_1 F_1}\right], \quad [33]$$

and $F_1 = \delta_1\gamma_G - 1$. Finally, the receiver pressure is obtained from [2] and [20] as

$$\bar{P}_2 = \bar{T}_2\left[\frac{1 - \theta_1(0)}{\bar{\theta}_2^{-1} - \theta_1(0)}\right]\left[\frac{\bar{\phi}_2^{-1} - \phi_1}{1 - \phi_1}\right]. \quad [34]$$

Equations [28]–[34] involve $\bar{\theta}_1$ in addition to nine parameters describing the initial state of the system. Some of these parameters can be related using [2] and [20] so that in effect only eight dimensionless parameters are independent. These can be related by

$$\bar{\rho}_2(0) = \frac{\bar{P}_2(0)}{\bar{T}_2(0)}\left[\frac{1 - \theta_1(0)\bar{\theta}_2(0)}{1 - \theta_1(0)}\right]\left[\frac{1 - \phi_1}{1 - \phi_1\bar{\phi}_2(0)}\right], \quad [35]$$

except when $\bar{P}_2(0) = 0$ and there are particles present in the receiver [since $\phi_2(0)$ is unity in this limit], in which case

$$\bar{\rho}_2(0) = \phi_1\bar{\theta}_2(0). \quad [36]$$

The system of equations [28]–[36] describe the state of the adiabatic system at all times in terms of $\bar{\theta}_1$. At pressure equilibrium, where $\bar{P}_1 = \bar{P}_2$, we can write

$$\left[\frac{1-\theta_1(0)}{\bar{\theta}_1^{-1}-\theta_1(0)}\right]^{\gamma_1} = \frac{[1-\theta_1(0)][1-\bar{\theta}_1+\alpha\bar{V}_2][1+\beta\bar{V}_2\bar{T}_2(0)]}{[1-\bar{\theta}_1+\alpha\bar{V}_2]+[\bar{V}_2(1-\theta_2(0))-\theta_1(0)][1-\bar{\theta}_1+\beta\bar{V}_2]+[(\beta-\alpha)\bar{V}_2\theta_1(0)\bar{\theta}_1]}, \quad [37]$$

where

$$\alpha = \rho'\left[\frac{1-\theta_2(0)}{1-\theta_1(0)}\right] \quad [38]$$

and

$$\beta = \bar{\rho}_2(0)\left[\frac{1+\phi_2(0)F_1}{1+\phi_1 F_1}\right], \quad [39]$$

which appear to have more mathematical then physical significance. They are clearly pseudo-density ratios; e.g. α is the gas density ratio which would occur if gas occupied the entire reservoirs rather than just the void volumes.

Now [37] can be solved for $\bar{\theta}_1 = \bar{\theta}_1(t_{eq})$ to obtain the adiabatic end-state analogous to the isothermal expression given by [27]. There is an advantage obtained by using γ_1 as a parameter rather than δ_1. When [9] is used to replace δ_1 by γ_1, and [35] is used to eliminate $\bar{\phi}_2(0)$ from [39],

$$\beta = \alpha\left(\frac{\gamma_1-1}{\gamma_G-1}\right)+\bar{\theta}_2(0)\left(\frac{\gamma_G-\gamma_1}{\gamma_G-1}\right) \quad [40]$$

so that all explicit mass fraction dependence has been removed from the solution to [37]. That is, any combination of ϕ_1 and δ_1 which yields γ_1 for a given γ_G is allowed without altering $\bar{\theta}_1(t_{eq})$, when $\theta_1(0)$, $\theta_2(0)$, $\bar{P}_2(0)$, $\bar{T}_2(0)$ and $\bar{V}_2$ are specified (fixed parameters). If instead, $\bar{\theta}_2(0)$ is eliminated via [35],

$$\beta = \alpha\left[1-\left(\frac{\gamma_G-\gamma_1}{\gamma_G-1}\right)\left(\frac{1-\bar{\phi}_2(0)}{1-\phi_1\bar{\phi}_2(0)}\right)\right] \quad [41]$$

and then explicit ϕ_1 dependence is removed only if $\bar{\phi}_2(0) \equiv 1$ or $\bar{\phi}_2(0) \ll 1$, although it appears to be weak unless $\bar{\phi}_2(0) > 1$. These cases prove to be very useful in limiting examples. Generally, a numerical solution of [37] is required; however, there are some useful special cases where exact results can be obtained. These limiting expressions are given in the appendix. Additional detailed results from them and further discussion can be found in Chenoweth & Paolucci (1990a).

4. CRITICAL PARAMETERS

In order to be able to determine if the flow is sonic and the sonic flow rate, the determination of critical parameters is necessary. It is assumed that the flow control point is located at the minimum area between the supply and receiver vessels. The transfer between vessels is treated in a quasi-steady fashion, in the sense that the steady, integrated Euler equation is applied across the flow control region at each instant of time as in pure gas analyses. The gas in the reservoirs is taken to remain stagnant at all times compared to the minimum area flow velocity.

Since viscous effects are neglected here, the one-dimensional steady Euler equation

$$u\,\mathrm{d}u = -\frac{\mathrm{d}P}{\rho} \quad [42]$$

can be written in integrated form as

$$u^2 - u_1^2 = 2\frac{P_1}{\rho_1}\left\{\theta_1\left(1-\frac{P}{P_1}\right)+(1-\theta_1)\left(\frac{\gamma_1}{\gamma_1-1}\right)\left[1-\left(\frac{P}{P_1}\right)^{1-1/\gamma_1}\right]\right\}. \quad [43]$$

The above equation gives the velocity u at any point where the pressure is P in terms of the supply reservoir conditions, indicated by the subscript 1. Equation [43] was given by Tangren *et al.* (1949). They show that it contains the pure gas isentropic expansion as well as the incompressible Bernoulli equation in the limiting cases of $\theta_1 \to 0$ and $\theta_1 \to 1$, respectively.

The sound speed can also be written in terms of the pressure ratio P/P_1 as

$$a^2 = \left[\frac{\gamma_1 P_1}{(1-\theta_1)\rho_1}\right]\left(\frac{P}{P_1}\right)^{1-1/\gamma_1}\left[1-\theta_1+\theta_1\left(\frac{P}{P_1}\right)^{1/\gamma_1}\right]^2, \quad [44]$$

so that when $u_1^2 \ll u^2$, $u^2 = a^2$ and $P = P_*$, the critical pressure ratio

$$K = \frac{P_*}{P_1} \quad [45]$$

is related to γ_1 and θ_1 by

$$\theta_1(\gamma_1-1)\left[1-(1+\gamma_1)K-\frac{\gamma_1}{2}\left(\frac{\theta_1}{1-\theta_1}\right)K^{1+1/\gamma_1}\right]+(1-\theta_1)\gamma_1\left[1-\left(\frac{1+\gamma_1}{2}\right)K^{1-1/\gamma_1}\right]=0. \quad [46]$$

The above equation shows that K is not constant, but may change rapidly with θ_1 (except when $\theta_1 \ll 1$) during the transfer. Equation [46] is valid for arbitrary γ_1 and is more general than the expression

$$\left(1+\frac{K\theta_1}{1-\theta_1}\right)^2 \approx 2\left[\frac{\theta_1}{1-\theta_1}(1-K)-\ln K\right], \quad [47]$$

given by Tangren *et al.* (1949), which is only valid for $\gamma_1 \to 1$. They tabulated the results for $1/3 \leqslant \theta_1 \leqslant 0.952$ since their interest was in a mixture of small gas bubbles in water. The more general results given by [46] are shown in figure 4 for $1 \leqslant \gamma_1 \leqslant 5/3$ and $0 \leqslant \theta_1 \leqslant 1$. In figure 4, K/K_0 is plotted vs θ_1 with γ_1 as the parameter, where

$$K_0 = \left(\frac{2}{\gamma_1+1}\right)^{\gamma_1/(\gamma_1-1)} \quad [48]$$

corresponds to the negligible volume fraction limit for K when $\theta_1 \ll 1$, which reduces to the pure gas value only if $\phi_1 \ll 1$ is also present. Note that with this normalization $0 \leqslant K/K_0 \leqslant 1$. We observe that although there is significant dependence on γ_1, it is not a large effect.

In order to obtain explicit analytical results, K/K_0 can be expanded in θ_1 and $(\gamma_1 - 1)$ as

$$K = K_0[1 + \bar{A}_1\theta_1 + \bar{A}_2\theta_1^2 + \ldots], \quad [49]$$

where

$$\bar{A}_1 = [1-(1+\gamma_1)K_0] \quad [50]$$

and

$$\bar{A}_2 = 4[K_0^{1/\gamma_1} + b_0 + b_1(\gamma_1-1) + b_2(\gamma_1-1)^2 + \ldots]. \quad [51]$$

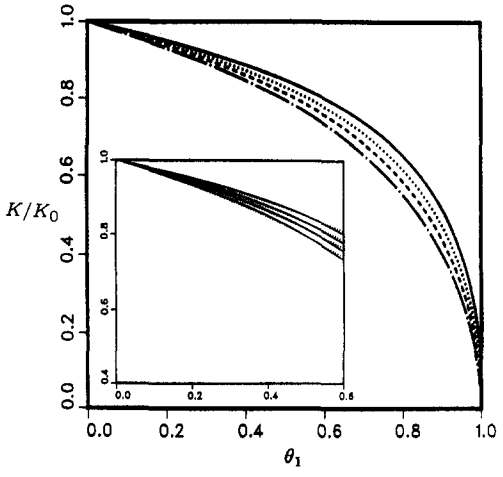

Figure 4. Critical pressure ratio vs supply volume fraction with γ_1 as the parameter; the inset is a comparison with [49]: ——, $\gamma_1 = 1$; ·····, $\gamma_1 = 1.2$; – – – –, $\gamma_1 = 7/5$; — · — ·, $\gamma_1 = 5/3$.

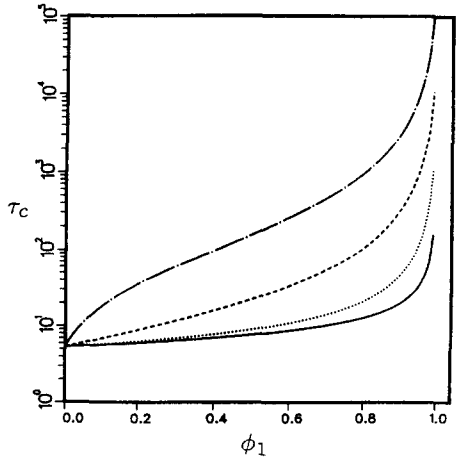

Figure 5. Sonic time scale factor vs supply mass fraction for $\gamma_G = 5/3$ with δ_1 as the parameter: ——, $\delta_1 = 10^{-2}$; ·····, $\delta_1 = 10^{-1}$; – – – –, $\delta_1 = 1$; — · — ·, $\delta_1 = 10$.

An accurate approximation is obtained for $\theta_1 \leqslant 0.6$ if the expansions are truncated above the quadratic terms, and the coefficients are adjusted such that $b_0 = -0.6505$, $b_1 = -0.0941$ and $b_2 = 0.0213$. The inset in figure 4 gives the approximate results [49]–[51] as dotted curves for the same γ_1 values used on the larger figure and given now as solid curves to show that the approximation is sufficiently accurate to be used for analytical purposes if $\theta_1 \leqslant 0.6$.

The other relevant critical parameters can be expressed in terms of K, γ_1 and θ_1 as follows:

$$\phi_*/\phi_1 = 1, \quad T_*/T_1 = K^{1-1/\gamma_1}, \quad r_*/r_1 = K^{1/\gamma_1}, \quad \theta_*/\theta_1 = [\theta_1 + (1-\theta_1)K^{-1/\gamma_1}]^{-1},$$
$$a_*/a_1 = [(1-\theta_1) + \theta_1 K^{1/\gamma_1}]K^{(\gamma_1-1)/2\gamma_1}, \quad \rho_* a_*/\rho_1 a_1 = K^{(\gamma_1+1)/2\gamma_1}. \qquad [52]$$

5. TRANSIENT RESULTS

Bounding end-state results for several transfer conditions are presented in the appendix. In the preceding section we presented the critical flow properties necessary to determine the sonic transfer rate as well as specifying when the transfer is in fact sonic. In this section transient results are obtained, and the time scale t_{eq} which relates to the previous results in the adiabatic limit is found. In addition to assuming the reservoirs stagnant during the transfer compared with the minimum flow area velocity, the transfer region is assumed to consist of negligible volume relative to the smaller of V_1 and V_2 for the vessels.

Since $\bar{\theta}_1 = \bar{\rho}_1$, the time rate of change of the supply volume fraction is

$$\frac{d\bar{\theta}_1}{d\tau} = -\bar{\rho}_e \bar{u}_e \left(\frac{\bar{V}_2}{1+\bar{V}_2}\right), \qquad [53]$$

where the velocity at the minimum flow area A_e

$$\bar{u}_e = \frac{u_e}{a_{G1}(0)}, \qquad [54]$$

and the non-dimensional time,

$$\tau = \left[\frac{A_e a_{G1}(0)}{V_2}\right](1+\bar{V}_2)t, \qquad [55]$$

are scaled by the initial supply gas sound speed. A more natural scaling which occurs involves the initial supply mixture sound speed, but the gas value is used here to better show the large effect which the presence of particles have on the actual transfer times. The reason for including $\bar{V}_2$ in the time scaling becomes obvious when the limits $\bar{V}_2 \ll 1$ and $\bar{V}_2 \gg 1$ are considered. The non-dimensional mass flux can be evaluated using [4], [5], [28], [29], [43] and [52], assuming $\bar{u}_1^2 \ll \bar{u}_e^2$:

$$\bar{\rho}_e \bar{u}_e = \left[\frac{\bar{\theta}_1}{\theta_1 + (1-\theta_1)y^{-1/\gamma_1}}\right]\left[2\frac{(1-\phi_1)}{\gamma_G}\left(\frac{\theta_1}{\theta_1(0)}\right)^{\gamma_1-1}\left(\frac{1-\theta_1(0)}{1-\theta_1}\right)^{\gamma_1-1}\right]^{\frac{1}{2}}$$
$$\left[(1-y)\left(\frac{\theta_1}{1-\theta_1}\right) + \left(\frac{\gamma_1}{\gamma_1-1}\right)(1-y^{1-1/\gamma_1})\right]^{\frac{1}{2}}, \qquad [56]$$

depending on the pressure ratio y so that

$$y = \begin{cases} K & \text{when } \dfrac{\bar{P}_2}{\bar{P}_1} \leqslant K, \\ \dfrac{\bar{P}_2}{\bar{P}_1} & \text{when } \dfrac{\bar{P}_2}{\bar{P}_1} > K, \end{cases} \qquad [57]$$

corresponding to the sonic or subsonic exit velocity at the minimum flow area. In general, [53] with [56] must be integrated, from $\bar{\theta}_1(0) = 1$ until $\bar{\theta}_1$ approaches the end-state $\bar{\theta}_1(t_{eq})$. At the same time [46] is solved for $K(\gamma_1, \theta_1)$, and $\bar{P}_2/\bar{P}_1$ is obtained via [28]–[36] so that y can be computed from [57]. Alternately, the approximate expression for K given by [49] can be used in [53] and [56] so that [53] can then be integrated directly for K while $\bar{P}_2/\bar{P}_1 \leqslant K$. In this sonic flow limit, the dimensional time history of $\bar{\theta}_1$ depends on four independent dimensionless parameters, γ_G, δ_1, ϕ_1 and $\theta_1(0)$,

which characterize the initial supply conditions. Note that although $\bar{V}_2$ appears via the scaling of τ, it is not present in the sonic dimensional time history. However, when $\bar{P}_2/\bar{P}_1 > K$, $\bar{V}_2$ enters, and three other independent parameters describing the initial receiver conditions must be selected from $\bar{T}_2(0)$, $\bar{P}_2(0)$, $\bar{\theta}_2(0)$ and $\bar{\phi}_2(0)$. Note that the fourth parameter is related to the other three via [35]. Since transient solutions must asymptotically approach the end-state results as $\tau \to \tau_{eq}$, the need for eight independent dimensionless parameters is consistent with the requirement previously found necessary to compute the end-state. From figure 4 it is clear that increasing the supply volume fraction enlarges the subsonic region in pressure ratio space for a given γ_1, whereas the opposite is true for increasing the supply mass fraction for a fixed θ_1.

5.1. Negligible Particle Volume Fraction

When $\theta_1(0) \ll 1$, then

$$\frac{d[\bar{\theta}_1^{(1-\gamma_1)/2}]}{d\tau} = \left\{(1-\phi_1)\left(\frac{\gamma_1-1}{2}\right)\left(\frac{\gamma_1}{\gamma_G}\right)[1-y^{(\gamma_1-1)/\gamma_1}]\right\}^{\frac{1}{2}}\left(\frac{\bar{V}_2}{1+\bar{V}_2}\right)y^{1/\gamma_1}. \quad [58]$$

5.1.1. Sonic solution

The above equation has the sonic or choked flow solution

$$\bar{\theta}_1 = \left[1+\left(\frac{\bar{V}_2}{1+\bar{V}_2}\right)\frac{\tau}{\tau_c}\right]^{2/(1-\gamma_1)}, \quad [59]$$

when $y = K \to K_0$, where the time scale factor

$$\tau_c^{-1} = (1-\phi_1)^{\frac{1}{2}}\left(\frac{\gamma_1}{\gamma_G}\right)^{\frac{1}{2}}\left(\frac{\gamma_1-1}{2}\right)\left(\frac{2}{\gamma_1+1}\right)^{(\gamma_1+1)/2(\gamma_1-1)} \quad [60]$$

reduces to the well-known pure gas result if $\phi_1 \ll 1$ and $\phi_1\delta_1 \ll 1$ so that $\gamma_1 \to \gamma_G$. Since τ is the dimensionless gas time scale, then the effects of particles enter the solution via τ_c and the exponent $2/(1-\gamma_1)$; the polytropic exponent (adiabatic index) is specified by the mixture ratio of specific heats γ_1 in the supply which together with the supply mass fraction ϕ_1, determine the supply mixture sound speed relative to that of the gas. Figure 5 gives τ_c vs ϕ_1 with δ_1 as parameter for $\gamma_G = 5/3$, a form comparable to figure 1 for γ_1. It is obvious that transfer times much longer than those for a pure gas are easily obtained, since even when $\theta_1(0) \ll 1$ it is still possible for ϕ_1 and γ_1 to take on their normal range of values. In addition, if $\phi_2 = \phi_1$ and $\theta_2(0) \ll 1$,

$$\bar{\theta}_1 = \left[\frac{1+\bar{V}_2\bar{P}_2(0)}{1+\bar{V}_2\dfrac{\bar{P}_2}{\bar{P}_1}}\right]^{1/\gamma_1}. \quad [61]$$

When the minimum area flow first becomes subsonic (denoted by an asterisk) we have

$$\bar{\theta}_1(\tau_*) = \left[\frac{1+\bar{V}_2\bar{P}_2(0)}{1+\bar{V}_2K_0}\right]^{1/\gamma_1}, \quad [62]$$

where

$$\frac{\tau_*}{\tau_c} = \left\{\left[\frac{1+\bar{V}_2\bar{P}_2(0)}{1+\bar{V}_2K_0}\right]^{(1-\gamma_1)/2\gamma_1} - 1\right\}\left(\frac{1+\bar{V}_2}{\bar{V}_2}\right) \quad [63]$$

specifies the time at which this occurs.

5.1.2. Subsonic solutions

As noted, the subsonic solution requires additional information about the receiver conditions. Analytical results can be obtained in this case if $\theta_2(0) \ll 1$ and $\phi_2 = \phi_1$. Then using [61] for $\bar{\theta}_1$ and $y = \bar{P}_2/\bar{P}_1$, solutions can be obtained in the charging limit as well as the discharging limit.

(i) $\bar{V}_2 \ll 1$ (charging limit). In this limit $\bar{T}_1 \approx 1$, $\bar{P}_1 \approx 1$ and $\bar{\theta}_1 \approx 1$, a new variable w can be introduced such that

$$y = \bar{P}_2 = (1-w^2)^{\gamma_1/(\gamma_1-1)}. \quad [64]$$

The new variable w is bounded by

$$0 \leqslant w \leqslant w_* = \left(\frac{\gamma_1 - 1}{\gamma_1 + 1}\right)^{\frac{1}{2}} \quad [65]$$

and is the minimum flow area Crocco number. It physically represents the fraction of the total enthalpy converted to kinetic energy at that point. The non-dimensional time for the problem becomes

$$\tau = \left[\frac{A_e a_{G1}(0)}{V_2}\right] t \quad [66]$$

and then [58] can be integrated to give

$$\tau = \tau_0 + (w_0 - w)\tau_w, \quad [67]$$

where the subscript 0 identifies the starting subsonic conditions defined by

$$\tau_0 = \begin{cases} \tau_* & \text{when } \bar{P}_2(0) \leqslant K_0, \\ 0 & \text{when } \bar{P}_2(0) > K_0, \end{cases} \quad [68]$$

where K_0 is given by [48],

$$\frac{\tau_*}{\tau_c} = \left(\frac{\gamma_1 - 1}{2\gamma_1}\right)[K_0 - \bar{P}_2(0)] \quad [69]$$

and

$$w_0 = \begin{cases} w_* & \text{when } \bar{P}_2(0) \leqslant K_0, \\ [1 - \bar{P}_2(0)^{(\gamma_1 - 1)/\gamma_1}]^{\frac{1}{2}} & \text{when } \bar{P}_2(0) > K_0. \end{cases} \quad [70]$$

The time scale factor τ_w is related to τ_c by

$$\frac{\tau_w}{\tau_c} = \left(\frac{\gamma_1 - 1}{2}\frac{K_0}{w_*}\right). \quad [71]$$

At pressure equilibrium $\bar{P}_2 = 1$ and $w = 0$, so at that time

$$\tau_{eq} = \tau_0 + w_0 \tau_w \quad [72]$$

and the time-dependent solution is then given by

$$\bar{P}_2 = \left[1 - \left(\frac{\tau_{eq} - \tau}{\tau_w}\right)^2\right]^{\gamma_1/(\gamma_1 - 1)}, \quad [73]$$

$$\bar{\theta}_2 = \bar{\theta}_2(0) + \frac{1}{\gamma_1}[\bar{P}_2 - \bar{P}_2(0)] \quad [74]$$

and

$$\bar{T}_2 = \left\{\frac{\gamma_1 \bar{P}_2}{\bar{P}_2 + \bar{P}_2(0)\left[\frac{\gamma_1}{\bar{T}_2(0)} - 1\right]}\right\}. \quad [75]$$

Note that when the receiving vessel is initially evacuated $\bar{T}_2 \to \gamma_1$. Of course, for solutions where $\bar{P}_2(0) < K_0$, the subsonic solution [73] must be mated with the sonic solution

$$\bar{P}_2 = \bar{P}_2(0) + \left(\frac{2\gamma_1}{\gamma_1 - 1}\right)\frac{\tau}{\tau_c} \quad [76]$$

at $\bar{P}_2 = K_0$. Results for the time of adiabatic pressure equilibrium and the receiver volume fraction are given in figures 6(a) and 6(c), respectively, for various γ_1 and $\bar{P}_2(0)$ parameter values. Only the subsonic portion of the $\bar{P}_2$ or $\bar{\theta}_2$ solutions is non-linear in time. This form of the results is useful, since when δ_1, ϕ_1 and γ_G are given, γ_1 is found from figure 1 or [9] and τ_c is obtained from figure 5 or [60]; then for a given $\bar{P}_2(0)$, actual times can be associated with the results when A_e, $a_{G1}(0)$ and V_2 are provided using [66], and θ_2 is found once $\theta_1(0)$ and $\theta_2(0)$ are selected. Notice that the greatest sensitivity to γ_1 occurs for $\bar{P}_2(0) \ll 1$.

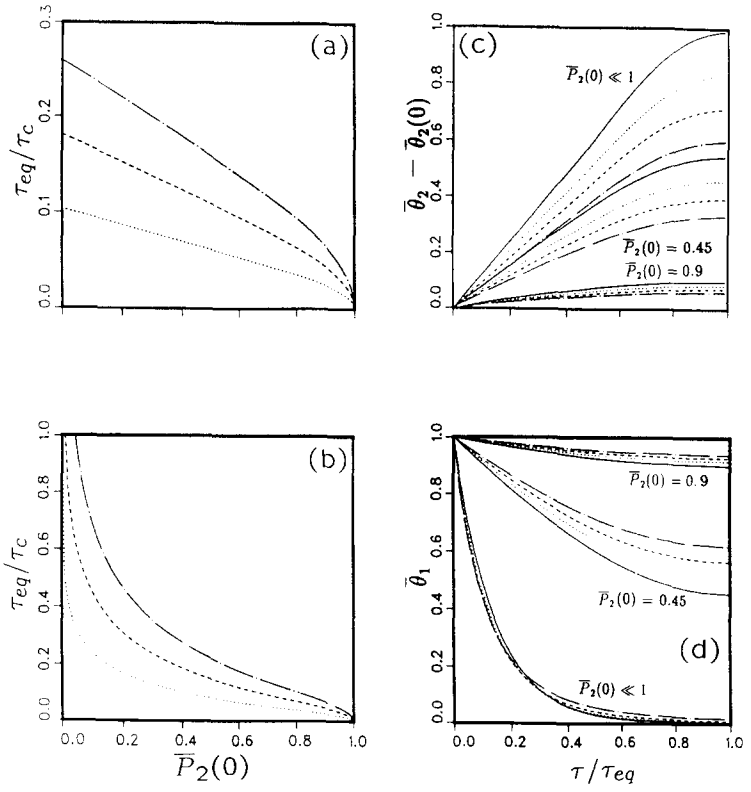

Figure 6. Time of adiabatic pressure equilibrium vs initial pressure ratio for $\theta_1(0) \ll 1$ and $\theta_2(0) \ll 1$ with γ_1 as the parameter for (a) $\bar{V}_2 \ll 1$ and (b) $\bar{V}_2 \gg 1$, and the corresponding volume fraction vs time with γ_1 and $\bar{P}_2(0)$ as parameters for (c) $\bar{V}_2 \ll 1$ and (d) $\bar{V}_2 \gg 1$: ——, $\gamma_1 = 1$; ·····, $\gamma_1 = 1.2$; – – – –, $\gamma_1 = 7/5$; — · — ·, $\gamma_1 = 5/3$.

(ii) $\bar{V}_2 \gg 1$ (discharging limit). In this discharging limit $\bar{T}_2 = \bar{T}_2(0)$, $\bar{P}_2 = \bar{P}_2(0)$ and $\bar{P}_1 = \bar{\theta}_1 \bar{T}_1 = \bar{\theta}_1^{\gamma_1}$, so that by defining a new variable z proportional to the minimum area Mach number we can write the pressure ratio as

$$y = \bar{P}_2(0)\bar{\theta}_1^{-\gamma_1} = (1 + z^2)^{\gamma_1/(1-\gamma_1)}, \tag{77}$$

so that [58] can then be integrated to give

$$\tau = \tau_0 + (I_{n_0} - I_n)\tau_*, \tag{78}$$

where

$$I_n = \int (1 + z^2)^{n/2}\, dz, \tag{79}$$

$$\tau_0 = \begin{cases} \tau_* & \text{when } \bar{P}_2(0) \leqslant K_0, \\ 0 & \text{when } \bar{P}_2(0) > K_0, \end{cases} \tag{80}$$

$$z_0 = \begin{cases} \left(\dfrac{\gamma_1 - 1}{2}\right)^{\frac{1}{2}} & \text{when } \bar{P}_2(0) \leqslant K_0, \\ [\bar{P}_2(0)^{(1-\gamma_1)/\gamma_1} - 1]^{\frac{1}{2}} & \text{when } \bar{P}_2(0) > K_0, \end{cases} \tag{81}$$

and

$$\frac{n}{2} = \frac{2 - \gamma_1}{\gamma_1 - 1}. \tag{82}$$

The subscript 0 identifies the beginning subsonic conditions. The time required for the flow to unchoke is

$$\frac{\tau_*}{\tau_c} = \left(\frac{2}{\gamma_1 + 1}\right)^{\frac{1}{2}} \bar{P}_2(0)^{(1-\gamma_1)/2\gamma_1} - 1. \quad [83]$$

The time scale factor τ_z is related to τ_w by

$$\frac{\tau_z}{\tau_w} = \bar{P}_2(0)^{(1-\gamma_1)/2\gamma_1}. \quad [84]$$

At pressure equilibrium $\bar{P}_1 \to \bar{P}_2(0)$, $z \to 0$ and $I_n \to 0$, so that the time to pressure equilibrium is

$$\tau_{eq} = \tau_0 + I_{n_0}\tau_z, \quad [85]$$

and the time dependent solution is given by

$$\tau = \tau_{eq} - I_n\tau_z, \quad [86]$$

which allows τ to be calculated explicitly for any pressure ratio. Exact analytical results are obtained by using the recursion formula

$$I_n = \frac{1}{1+n}\{z(1+z^2)^{n/2} + nI_{n-2}\}, \quad [87]$$

with $n = 0, 1, 2, \ldots$, where $I_0 = z$, and $I_1 = \{z(1+z^2)^{\frac{1}{2}} + \ln[z + (1+z^2)^{\frac{1}{2}}]\}/2$ terminate the recursion for any positive even or odd integer value of n, respectively. The mixture ratio of specific heats is given by

$$\gamma_1 = \frac{n+4}{n+2}, \quad [88]$$

so that the results are valid at an infinite number of discrete values of $\gamma_1 = 2, 5/3, 6/4, 7/5, 8/6, \ldots$, which asymptotically approaches unity for large n.

Similar results were obtained for the pure gas case by Chenoweth (1974, section E), who gave explicit expressions only for $\gamma_G = 5/3$ and $7/5$. As opposed to the pure gas case, here the other values of γ_1 between γ_G and unity are more physically significant because γ_1 can actually reach all those values by a proper choice of ϕ_1.

These discharging results are given in figures 6(b) and 6(d) in a form similar to the charging case, where the time of adiabatic pressure equilibrium and the supply volume fraction are plotted vs $\bar{P}_2(0)$ and τ/τ_{eq}, respectively, for various values of γ_1 and $\bar{P}_2(0)$. Here $\tau_{eq} \to \infty$ as $\bar{P}_2(0) \to 0$. For charging, the greatest sensitivity of $\bar{\theta}_2$ to γ_1 occurred for $\bar{P}_2(0) \ll 1$, while here that limit for $\bar{\theta}_1$ shows the least sensitivity to γ_1 on the τ/τ_{eq} scale. However, due to the fact τ_{eq} has its greatest variation with γ_1 in that limit, there are still very large γ_1 effects present on the $\bar{\theta}_1$ dimensional time histories.

5.2. Isothermal Supply Choked Flow

When $\bar{P}_2/\bar{P}_1 \leqslant K$, the approximate expressions [48]–[51], truncated above the quadratic terms, may be used to integrate [53]–[57], provided $\theta_1(0) \leqslant 0.6$. This becomes particularly easy in the isothermal limit $\gamma_1 \to 1$ since then $K_0 = e^{-1/2}$, $\bar{A}_1 \approx -0.2131 = -\bar{a}$ and $\bar{A}_2 \approx -0.1760 = -\bar{b}$. At least one of the conditions $\gamma_G \to 1$, $\phi_1 \to 1$ or $\phi_1\delta_1 \gg 1$ must be true so that $\gamma_1 \to 1$. The resulting supply volume fraction is then given implicitly as a function of time by

$$\tau = \left(\frac{\gamma_G}{1-\phi_1}\right)^{\frac{1}{2}}\left(\frac{1+\bar{V}_2}{\bar{V}_2}\right)\left\{\bar{e}\ln\left[\left(\frac{1+\bar{c}\theta_1}{1+\bar{c}\theta_1(0)}\right)\left(\frac{1-\bar{d}\theta_1(0)}{1-\bar{d}\theta_1}\right)\right]\right.$$
$$\left. -\bar{f}\ln\left[\left(\frac{\theta_1}{\theta_1(0)}\right)^2\left(\frac{1-\bar{a}\theta_1(0)-\bar{b}\theta_1^2(0)}{1-\bar{a}\theta_1-\bar{b}\theta_1^2}\right)\right]\right\}, \quad [89]$$

where $\bar{c} = 0.3264$, $\bar{d} = 0.5394$, $\bar{e} = 1.7015$ and $\bar{f} = 0.8244$ specify the other constants. The point in time where [89] ceases to be valid (i.e. $\bar{P}_2/\bar{P}_1 = K$) is determined from

$$K \approx e^{-\frac{1}{2}}(1 - \bar{a}\theta_1 - \bar{b}\theta_1^2). \quad [90]$$

Figure 7 is a plot of $\bar{\theta}_1$ vs $\tau(1-\phi_1)^{1/2}\bar{V}_2/[\gamma_G^{1/2}(1+\bar{V}_2)]$ with $\theta_1(0)$ as a parameter. It shows that when $\theta_1(0)$ is not negligible, significant effects occur in this physically realistic limit. Obviously, these results are valid for all times in the limit of a sonic discharge to vacuum, $\bar{V}_2 \gg 1$ and $\bar{P}_2(0) \ll 1$, when $\gamma_1 \approx 1$. It does not appear that explicit analytical results are easily obtained in this limit in a form comparable to [89] when the flow is unchoked.

5.3. *Numerical Results*

The detailed transient solutions valid for $\theta_1(0) \ll 1$, $\theta_2(0) \ll 1$, $\bar{\phi}_2(0) = 1$ and $\bar{V}_2 \ll 1$ or $\bar{V}_2 \gg 1$ are very useful, but they leave a number of questions unanswered. In particular, what are the effects of non-negligible reservoir volume fractions, unequal reservoir mass fractions and reservoir volume ratios of the order of unity, both individually and in combination? These questions are examined in this section using exactly the same conditions previously used in the end-state calculations given in Chenoweth & Paolucci (1990a). That is, $\gamma_G = 5/3$ and $\gamma_1 = 7/5$. The same three cases, $\bar{\phi}_2(0) = 1$, $\bar{\phi}_2(0) \ll 1$ and $\theta_2(0) = 1/2$, are compared for various $\bar{V}_2$ and $\bar{P}_2(0)$ values for both $\theta_1(0) \ll 1$ and $\theta_1(0) = 1/2$ with $\bar{T}_2(0) = 1$. The results are then presented in the same form used for the special charging and discharging exact solutions already discussed. These are valid for any ϕ_1 and δ_1 giving $\gamma_1 = 7/5$ when $\gamma_G = 5/3$, similar to the end-state results.

First, the times of adiabatic pressure equilibrium are given in figures 8(a–f). Figure 8(a) is for $\bar{\phi}_2(0) = 1$ and $\theta_1(0) \ll 1$ so that $\alpha = \beta$ and the upper and lower curves are in fact the exact solutions; thus the only new information on this plot is the $\bar{V}_2 = 1$ and 3 curves. Notice that the $\bar{V}_2 = 1$ curve is much closer to the charging limit than it is to the discharging curve. In figure 8(b) we see that for the case where there is negligible particles $\bar{\phi}_2(0) \ll 1$ in the receiver initially, it appears that there is little difference from figure 8(a). In fact, even when $\theta_2(0) = 1/2$, from figure 8(c) we see that the upper curve for discharging appears to be the same; here the other curves are lowered as might be expected, since the gas volume ratio V' has been decreased. When $\bar{P}_2(0) < K$, there are two contributions to τ_{eq}: the time to unchoked flow τ_* and the time spent with subsonic flow. The sonic solution to [58] depends on γ_1, $\theta_1(0)$ and $(\tau/\tau_c)\bar{V}_2/(1+\bar{V}_2)$ so that it is independent of the receiver conditions which are being altered here. Obviously, any time the sonic portion dominates the subsonic portion, little effect of the receiver parameters will be observed. Also, since the subsonic portion of the solution approaches the end-state results at $t \to t_{eq}$, those end-state results give a good indication of the parameter dependence for the final part of the time histories. In the discharging limit, the end-state results for $\bar{\theta}_1(t_{eq})$ show a dependence only on γ_1, $\theta_1(0)$ and $\bar{P}_2(0)$. Thus, one would expect to observe only the dependence on $\theta_1(0)$ for τ_{eq}/τ_c in the $\bar{V}_2 \gg 1$ limit and independent of $\bar{\phi}_2(0)$ and $\bar{\theta}_2(0)$. Indeed, this is seen in figures 8(d–f) which are for $\theta_1(0) = 1/2$, where again the

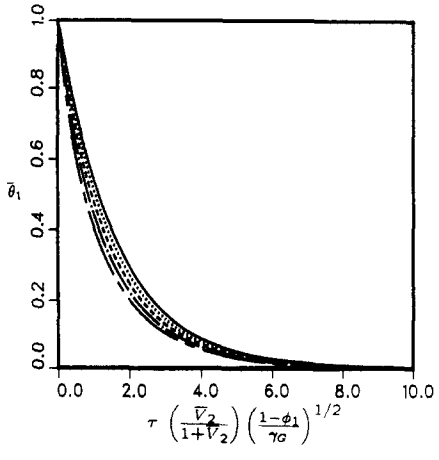

Figure 7. Supply volume fraction for sonic isothermal discharge vs normalized time with $\theta_1(0)$ as parameter when $\delta_1 \gg 1$: ——, $\theta_1(0) \ll 1$; ·····, $\theta_1(0) = 0.15$; – – – –, $\theta_1(0) = 0.3$; — · — ·, $\theta_1(0) = 0.45$; — — —, $\theta_1(0) = 0.6$.

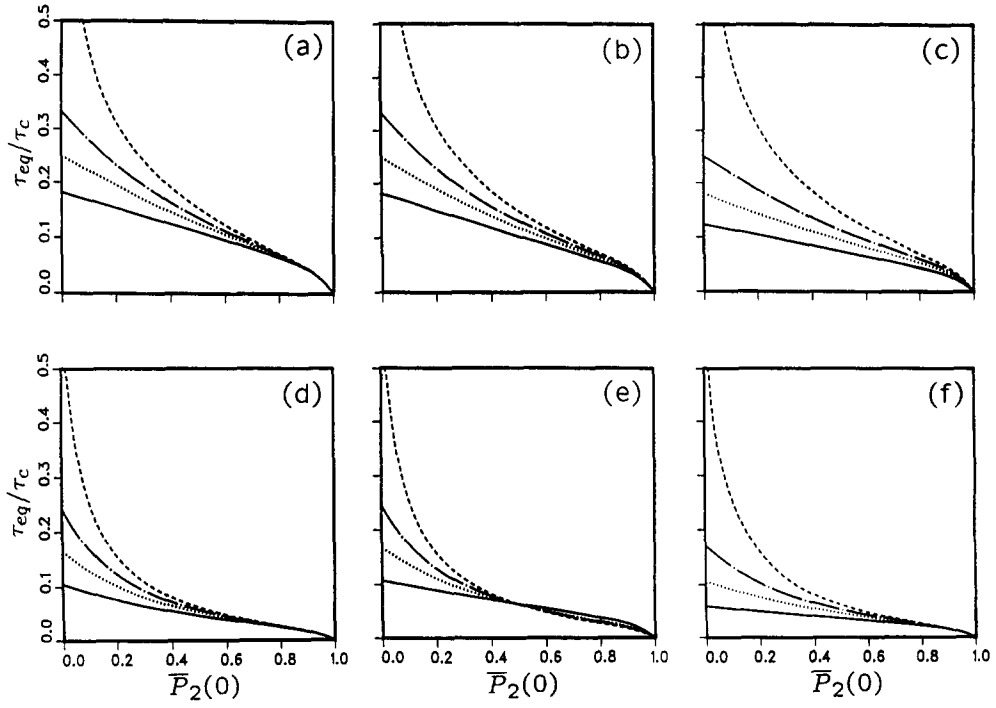

Figure 8. Time of adiabatic pressure equilibrium vs initial pressure ratio for $\gamma_G = 5/3$, $\gamma_l = 7/5$ and $\bar{T}_2(0) = 1$ with $\bar{V}_2$ as the parameter. $\theta_1(0) \ll 1$: (a) $\bar{\phi}_2(0) = 1$; (b) $\bar{\phi}_2(0) \ll 1$; (c) $\theta_2(0) = 1/2$. $\theta_1(0) = 1/2$: (d) $\bar{\phi}_2(0) = 1$; (e) $\bar{\phi}_2(0) \ll 1$; (f) $\theta_2(0) = 1/2$. ——, $\bar{V}_2 \ll 1$; ·····, $\bar{V}_2 = 1$; — · —, $\bar{V}_2 = 3$; – – – –, $\bar{V}_2 \gg 1$.

dashed curves appear to be the same but substantially different from the $\theta_1(0) \ll 1$ cases. In these figures all of the $\theta_1(0) = 1/2$ curves are substantially below the $\theta_1(0) \ll 1$ results. Thus, it appears that increasing the volume fractions decrease transfer times, while increasing mass fractions increase the transfer times via τ_c.

Time histories for $\bar{\theta}_1$ and $\bar{\theta}_2 - \bar{\theta}_2(0)$ are given in figures 9(a–c) –12(a–c) for the cases corresponding to those in figures 8(a–f), but for just two specific values of $\bar{P}_2(0)$; these values are $\bar{P}_2(0) = 1/2$ and 0.01, representing mostly subsonic flow, and flow which remains sonic for significant periods prior to the unchoking, respectively. The behavior just discussed for the discharging limit $\bar{V}_2 \gg 1$ is readily observable here; similarly, the sonic solution portions for $\bar{P}_2 < K$ display the behavior already discussed. This explains why there appears to be much less effect of $\bar{\phi}_2(0)$ and $\bar{\theta}_2(0)$ when $\bar{P}_2(0) = 0.01$ than for $\bar{P}_2(0) = 1/2$. Also, for $\bar{P}_2(0) = 0.01$ it appears that the histories in terms of τ/τ_{eq} are nearly independent of $\theta_1(0)$; thus the effects of $\theta_1(0)$ are primarily contained in the normalization of $\bar{\theta}_1$, $\bar{\theta}_2$, and τ/τ_{eq}. This is not the case for $\bar{P}_2(0) = 1/2$, where the entire flow is predominantly subsonic.

6. CONCLUSIONS

The equilibrium flow of homogeneous two-phase mixtures between two vessels with no phase change and an ideal carrier gas has been investigated. It is found that the mixture behaves similar to a polytropic Abel–Noble gas. The mixture thermodynamic properties, the end-state in each vessel at pressure equilibrium, the critical parameters and time-dependent results are given for adiabatic and isothermal limiting cases. The mass transferred at adiabatic pressure equilibrium can be substantially less than that when thermal equilibrium is also reached (see the appendix). It is also found that the adiabatic pressure equilibrium level may not be the same as that reached at thermal equilibrium. Furthermore, it is shown that the transfer times can be very slow compared to those of a pure gas, due to the large reduction possible in the mixture sound speed.

The results given here form the base solutions which can be used for comparisons as the more restrictive assumptions are removed. The limits of validity of these base solutions must be

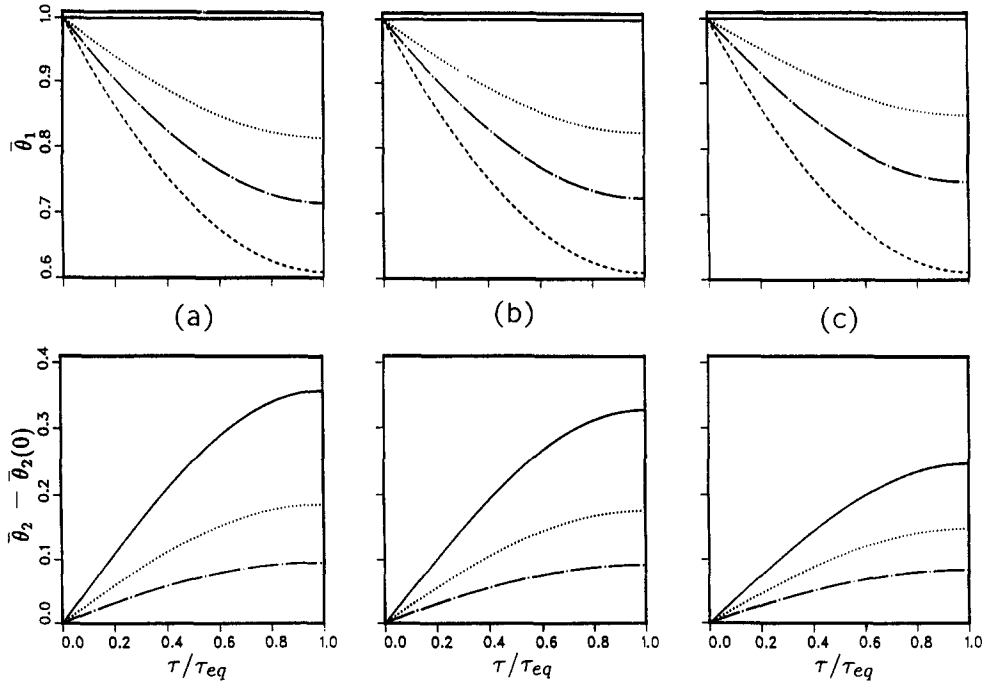

Figure 9. Volume fraction vs time for $\theta_1(0) \ll 1$ and $\bar{P}_2(0) = 1/2$ with $\bar{V}_2$ as the parameter for $\gamma_G = 5/3$, $\gamma_1 = 7/5$, $\bar{T}_2(0) = 1$ and (a) $\bar{\phi}_2(0) = 1$, (b) $\bar{\phi}_2(0) \ll 1$ and (c) $\theta_2(0) = 1/2$: ——, $\bar{V}_2 \ll 1$; ·····, $\bar{V}_2 = 1$; —·—, $\bar{V}_2 = 3$; – – – –, $\bar{V}_2 \gg 1$.

determined more rigorously than it was possible in this investigation. The end-state results do show the conditions under which finite reservoir heat transfer rates are necessary to determine mass transfer and pressure levels. The effects of a non-ideal carrier gas, non-zero mixture transport properties, phase change, thermal slip and relative velocity are beyond the scope of this study and

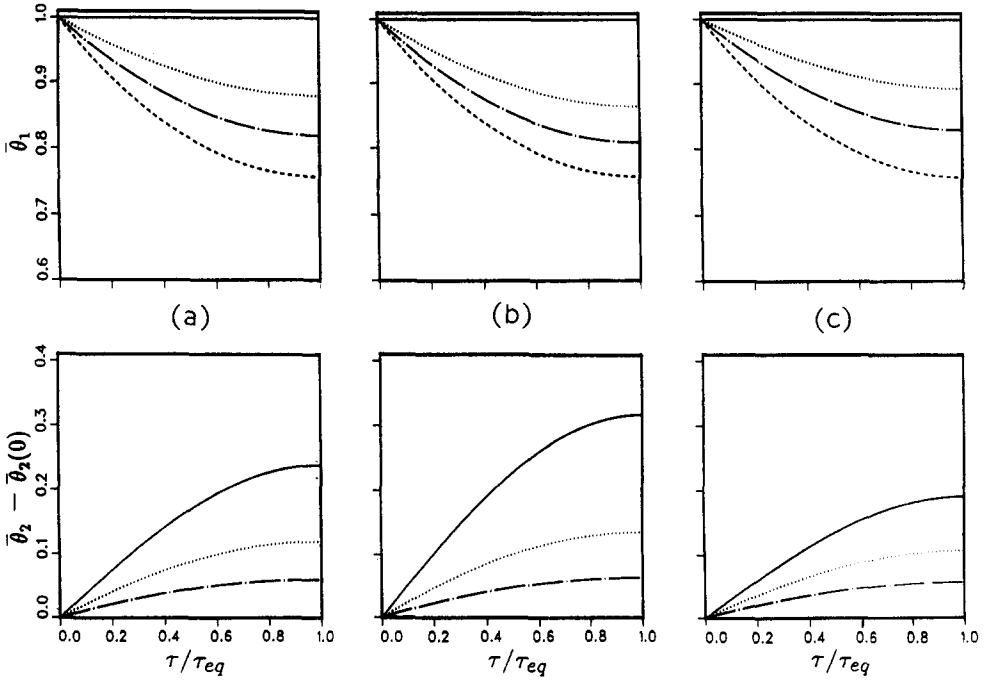

Figure 10. Volume fraction vs time for $\theta_1(0) = 1/2$ and $\bar{P}_2(0) = 1/2$ with $\bar{V}_2$ as the parameter for $\gamma_G = 5/3$, $\gamma_1 = 7/5$, $\bar{T}_2(0) = 1$ and (a) $\bar{\phi}_2(0) = 1$, (b) $\bar{\phi}_2(0) \ll 1$ and (c) $\theta_2(0) = 1/2$: ——, $\bar{V}_2 \ll 1$; ·····, $\bar{V}_2 = 1$; —·—, $\bar{V}_2 = 3$; – – – –, $\bar{V}_2 \gg 1$.

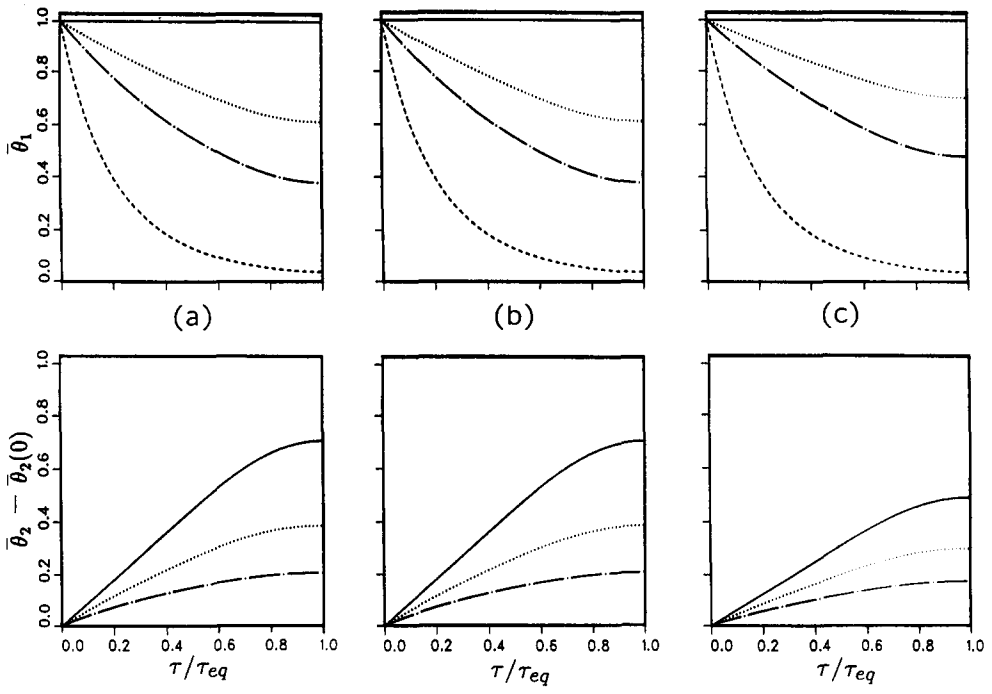

Figure 11. Volume fraction vs time for $\theta_1(0) \ll 1$ and $\bar{P}_2(0) = 0.01$ with $\bar{V}_2$ as the parameter for $\gamma_G = 5/3$, $\gamma_l = 7/5$, $\bar{T}_2(0) = 1$ and (a) $\bar{\phi}_2(0) = 1$, (b) $\bar{\phi}_2(0) \ll 1$ and (c) $\theta_2(0) = 1/2$: ——, $\bar{V}_2 \ll 1$; ·····, $\bar{V}_2 = 1$; —·—, $\bar{V}_2 = 3$; – – – –, $\bar{V}_2 \gg 1$.

must be examined in future investigations. In any event, the parameter dependence of the time to adiabatic pressure equilibrium should prove to be useful for scaling estimates even when many of the assumptions are not strictly valid. In the pure gas limit, such a result has been shown to be true in many cases.

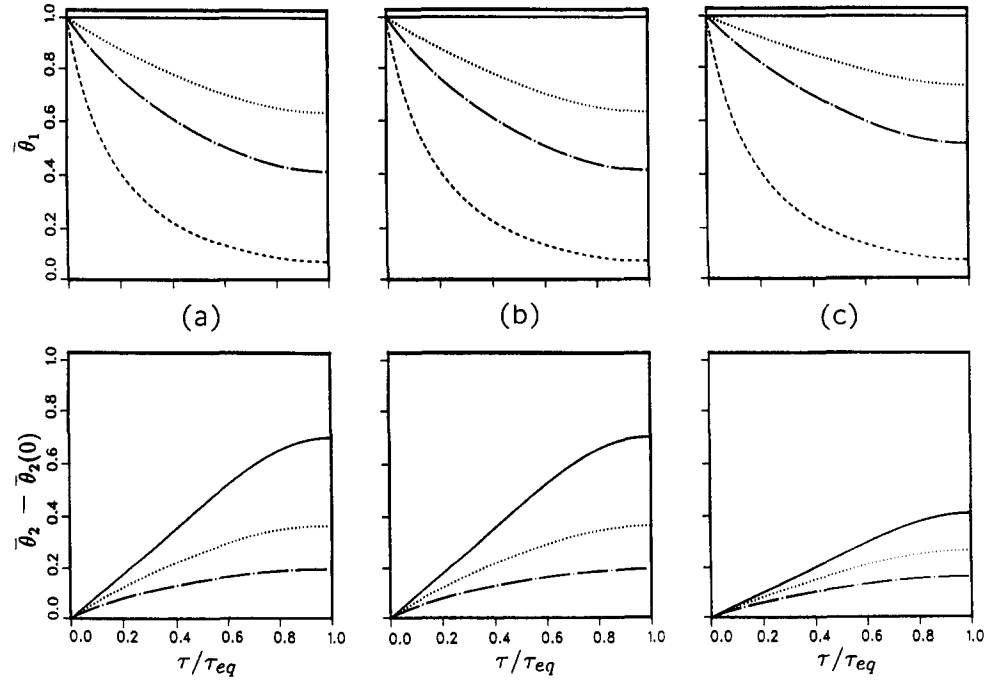

Figure 12. Volume fraction vs time for $\theta_1(0) = 1/2$ and $\bar{P}_2(0) = 0.01$ with $\bar{V}_2$ as the parameter for $\gamma_G = 5/3$, $\gamma_l = 7/5$, $\bar{T}_2(0) = 1$ and (a) $\bar{\phi}_2(0) = 1$, (b) $\bar{\phi}_2(0) \ll 1$ and (c) $\theta_2(0) = 1/2$: ——, $\bar{V}_2 \ll 1$; ·····, $\bar{V}_2 = 1$; —·—, $\bar{V}_2 = 3$; – – – –, $\bar{V}_2 \gg 1$.

Acknowledgement—This work was performed under the auspices of the U.S. Department of Energy by Sandia National Laboratories, Livermore, Calif., under Contract No. DE-AC04-76DP00789.

REFERENCES

ACKERET, J. 1930 Experimental and theoretical investigations on cavitation in water (translation). *Tech. Mech. Thermo-Dynam., Berl.* **1,** 63–72.

ARDRON, K. H. & DUFFEY, R. B. 1978 Acoustic wave propagation in a flowing liquid–vapor mixture. *Int. J. Multiphase Flow* **4,** 303–322.

CHENOWETH, D. R. 1974 Gas transfer analysis: sections A–F. Sandia National Labs Reports SAND74-8211, SAND74-8212, SAND74–8213, SAND74-8214, SAND74-8215 and SAND74-8216.

CHENOWETH, D. R. 1979 Gas transfer analysis: section G—gas flow in real duct systems. Sandia National Labs Report SAND79-8212.

CHENOWETH, D. R. 1983 Gas transfer analysis: section H—real gas results via the van der Waals equation of state and virial expansion extensions of its limiting Abel–Noble form. Sandia National Labs Report SAND83-8229.

CHENOWETH, D. R. & PAOLUCCI, S. 1989 On pressure change occurring during gas mixing. *Am. J. Phys.* **57,** 463–465.

CHENOWETH, D. R. & PAOLUCCI, S. 1990a Compressible flow of a multiphase fluid between two vessels. Part I—Ideal carrier gas. Sandia National Labs Report SAND90-8486.

CHENOWETH, D. R. & PAOLUCCI, S. 1990b Compressible flow of a two-phase fluid between finite vessels—II. Abel–Noble carrier gas. In preparation.

COLE, J. E. & DOBBINS, R. A. 1970 Propagation of sound through atmospheric fog. *J. atmos. Sci.* **27,** 426–434.

DAVIDSON, G. A. 1975 Sound propagation in fogs. *J. atmos. Sci.* **32,** 2201–2205.

GUENOCHE, H., BEN HADID, H., SEDES, C., LARINI, M. & RONDOT, C. 1988 Speed of sound in a two-phase gas–solid sphere mixture. I: experimental study. *J. Méc. théor. appl.* **7,** 859–874.

GUMEROV, N. A., IVANDAEV, A. I. & NIGMATULIN, R. I. 1988 Sound waves in monodisperse gas–particle or vapour–droplet mixtures. *J. Fluid Mech.* **193,** 53–74.

HEINRICH, G. 1942 Uber strömungen von schäumen. *Z. angew. Math. Mech.* **22,** 117–118.

HENRY, R. E. & GROLMES, M. A. 1971 Pressure-pulse propagation in two-phase one- and two-component mixtures. Argonne National Labs Report ANL-7792.

KARPLUS, H. B. 1958 The velocity of sound in a liquid containing gas bubbles. Armour Research Fdn Report C00-248.

KARPLUS, H. B. 1961 Propagation of a pressure wave in a mixture of water and steam. Armour Research Fdn Report 4132-12.

MARBLE, F. E. 1970 Dynamics of dusty gases. *A. Rev. Fluid Mech.* **2,** 397–446.

NGUYEN, D. L., WINTER, E. R. F. & GREINER, M. 1981 Sonic velocity in two-phase systems. *Int. J. Multiphase Flow* **7,** 311–320.

RUGGLES, A. E., LAHEY, R. T. JR, DREW, D. A. & SCARTON, H. A. 1988 An investigation of the propagation of pressure perturbations in bubbly air/water flows. *J. Heat Transfer* **110,** 494–499.

SCHMITT-VON SCHUBERT, B. 1969 Schallwellen in gasen mit festen teilchen. *Z. angew. Math. Phys.* **20,** 922–935.

SEMENOV, N. I. & KOSTERIN, S. I. 1964 Results of studying the speed of sound in moving gas–liquid systems. *Teploenergetika* **11,** 46–51.

SEWELL, S. J. T. 1910 On the extinction of sound in a viscous atmosphere by small obstacles of cylindrical and spherical form. *Phil. Trans. R. Soc., Lond.* **A210,** 239–270.

SILBERMAN, E. 1957 Sound velocity and attenuation in bubbly mixtures measured in standing wave tubes. *J. acoust. Soc. Am.* **29,** 925–933.

SOO, S. L. 1960 Effect of transport processes on attenuation and dispersion in aerosols. *J. acoust. Soc. Am.* **32,** 943–946.

STEEN, B. 1986 An acoustic method of measuring particle mass concentration in gases. *J. Aerosol Sci.* **17,** 485–488.

TANGREN, R. F., DODGE, C. H. & SEIFERT, H. S. 1949 Compressibility effects in two-phase flow. *J. appl. Phys.* **20,** 637–645.

TEMKIN, S. & DOBBINS, R. A. 1966a Attenuation and dispersion of sound by particulate–relaxation processes. *J. acoust. Soc. Am.* **40,** 317–324.

TEMKIN, S. & DOBBINS, R. A. 1966b Measurements of attenuation and dispersion of sound by an aerosol. *J. acoust. Soc. Am.* **40,** 1016–1024.

VAN WIJNGAARDEN, L. 1972 One-dimensional flow of liquids containing small gas bubbles. *A. Rev. Fluid Mech.* **4,** 369–396.

WALLIS, G. B. 1969 *One-dimensional Two-phase Flow.* McGraw-Hill, New York.

WOOD, A. B. 1941 *A Textbook of Sound,* 2nd edn. Bell, London.

WOOD, A. B. 1955 *A Textbook of Sound,* 3rd edn. Macmillan, New York.

ZINK, J. W. & DELSASSO, L. P. 1958 Attenuation and dispersion of sound by solid particles suspended in a gas. *J. acoust. Soc. Am.* **30,** 765–771.

APPENDIX

A Number of Limiting Solutions to [37] for the Adiabatic End-state

$\gamma_l \to 1$ (isothermal limit)

There are three independent ways to cause $\gamma_1 \to 1$: $\gamma_G \to 1$, $\phi_1 \to 1$ and $\phi_1 \delta_1 \gg 1$. When $\gamma_1 \to 1$ (supply vessel isothermal), [37] becomes quadratic in $\bar{\theta}_1(t_{eq})$. The case $\gamma_G \to 1$ results in the trivial no flow limit $\bar{\theta}_1(t_{eq}) \to 1$. The no flow limit also occurs whenever $\bar{P}_2(0) \to 1$, $\bar{V}_2 \to 0$ or $\theta_2(0) \to 1$. For $\phi_1 \to 1$ or $\phi_1 \delta_1 \gg 1$, the non-trivial solution $\bar{\theta}_1(t_{eq}) = \bar{\theta}_1(\infty)$ results, where $\bar{\theta}_1(\infty)$ is given by [27]. In this case

$$\bar{P}_1(t_{eq}) = \left(\frac{1 + \rho' V'}{1 + V'}\right), \qquad [A.1]$$

which is the same as that given by [24] only when $\bar{T}(\infty) = 1$.

$V' \ll 1$ (charging limit)

When the initial receiver gas volume is much smaller than the initial supply gas volume, the supply conditions will remain essentially unchanged during the charging of the receiver to the supply pressure level, so that $\bar{P}_1 \approx 1$ and $\bar{\theta}_1 \approx 1$.

The conditions in the receiver do change and can be investigated via [28]–[35] if the limiting results are carefully derived. The procedures and results are similar to those of a pure gas [see Chenoweth (1974, sections C and D)]. When $\phi_2 = \phi_1$ and using $\bar{P}_2(t_{eq}) = 1$,

$$\bar{\theta}_2(t_{eq}) = \bar{\theta}_2(0) + \left[\frac{1 - \bar{P}_2(0)}{\gamma_1}\right][1 - \theta_1(0)\bar{\theta}_2(0)] \qquad [A.2]$$

and

$$T_2(t_{eq}) = \left\{\frac{\gamma_1 - \theta_1(0)(1 - \bar{P}_2(0))}{1 + \bar{P}_2(0)\left[\dfrac{\gamma_1}{\bar{T}_2(0)} - 1\right] - \theta_1(0)[1 - \bar{P}_2(0)]}\right\}. \qquad [A.3]$$

When the receiving vessel is initially evacuated $\bar{T}_2(t_{eq}) \to [\gamma_1 - \theta_1(0)]/[1 - \theta_1(0)]$. This limit gives the maximum effect of compressive heating during the charging process, which for a pure gas reduces to the well-known result of γ_G. Clearly, temperatures exceeding the pure gas limit are possible when $\theta_1(0) \neq 0$. Also notice from [A.2] that when an evacuated vessel, initially containing no particles, is used to rapidly draw a sample from its surroundings, the sample volume fraction may be less than that of its surroundings by a factor as large as γ_1^{-1}.

$V' \gg 1$ (discharging limit)

In this limit the receiver conditions remain essentially unchanged, so that the supply discharges to the receiver pressure level. Therefore from [28] or [37] we obtain the supply volume fraction at the adiabatic pressure equilibrium $\bar{P}_1(t_{eq}) = \bar{P}_2(0)$:

$$\bar{\theta}_1(t_{eq}) = \{\theta_1(0) + [1 - \theta_1(0)]\bar{P}_2(0)^{-1/\gamma_1}\}^{-1}. \quad [A.4]$$

For a pure gas this limit is given by Chenoweth (1974, sections E and H).

$\alpha = \beta$ (single fluid or negligible particle heat capacity limit)

Another solution of [37] occurs when $\alpha = \beta$, giving

$$\bar{\theta}_1(t_{eq}) = \{\theta_1(0) + [1 - \theta_1(0)]\bar{P}_1(t_{eq})^{-1/\gamma_1}\}^{-1}, \quad [A.5]$$

where

$$\bar{P}_1(t_{eq}) = \left[\frac{1 + V'\bar{P}_2(0)}{1 + V'}\right]; \quad [A.6]$$

then $\bar{P}_1(t_{eq}) = \bar{P}(\infty)$ only if $\bar{T}(\infty) = \bar{T}_2(0) = 1$. This special solution can occur in three ways:

(a) receiver initially evacuated with no particles, $\bar{P}_2(0) = 0$, $\theta_2(0) = \phi_2(0) = 0$;
(b) mass fraction of particles the same in each vessel (single fluid) $\phi_1 = \phi_2(0)$; or
(c) particle heat capacity negligible versus that of the gas, $\delta_1 \ll 1$, $\gamma_1 \to \gamma_G$.

Obviously cases (a) and (b) both result in single fluid transfer problems. For case (a) $\alpha = \beta = 0$, while for cases (b) and (c) we have

$$\alpha = \beta = \rho'\left[\frac{1 - \theta_2(0)}{1 - \theta_1(0)}\right]. \quad [A.7]$$

In the limiting solutions given above, $\bar{\theta}_1(t_{eq}) \neq \bar{\theta}_1(\infty)$ except for very special cases. In order to examine the magnitude of the difference, a defect parameter is defined analogous to that defined by Chenoweth (1974, section A; 1983, section H):

$$\Delta \equiv \frac{\bar{\theta}_1(t_{eq}) - \bar{\theta}_1(\infty)}{1 - \bar{\theta}_1(\infty)}. \quad [A.8]$$

Since $\bar{\theta}_1 = \bar{\rho}_1$, this parameter represents the maximum fraction of the mass transferred at thermal equilibrium, which may be retained in the supply when pressure equilibrium is first reached. This mass defect is due to departures from thermal equilibrium and can be bounded in some cases. For example, using [27] and [A.5] in [A.8] when $\bar{T}_2(0) = 1$ so that $\bar{P}_1(t_{eq}) = \bar{P}(\infty)/\bar{T}(\infty)$ when $\alpha = \beta$, we get

$$\Delta = \frac{\bar{P}_1(t_{eq})^{1/\gamma_1} - \bar{P}_1(t_{eq})}{[1 - \bar{P}_1(t_{eq})]\{1 - \theta_1(0)[1 - \bar{P}_1(t_{eq})^{1/\gamma_1}]\}}, \quad [A.9]$$

which is bounded by

$$\Delta_0 \leqslant \Delta \leqslant \Delta_1 = \frac{\Delta_0}{\bar{P}_1(t_{eq})^{1/\gamma_1}}. \quad [A.10]$$

The subscript on Δ refers to the values of $\theta_1(0)$. That is, for all $0 \leqslant \theta_1(0) \leqslant 1$, Δ is always greater than that of pure gas ($\theta_1(0) = 0$) for any given $\bar{P}_1(t_{eq})$. For $\theta_1(0) \leqslant 1/2$, a lower upper bound can be obtained:

$$\Delta \leqslant \Delta_{1/2} \leqslant 1 - 1/\gamma_1. \quad [A.11]$$

The value $1 - 1/\gamma_1$ is approached for all $\theta_1(0)$, when $\bar{P}_1(t_{eq})$ (given by [A.6]) approaches unity; clearly this is possible only when $V' \ll 1$ or $\bar{P}_2(0) \to 1$. When $\gamma_1 \to \gamma_G$ and $V' \to \bar{V}_2$, the results agree with those for a pure gas given by Chenoweth (1974, section A; 1983, section H). For $1/2 \leqslant \theta_1(0) < 1$, a maximum value occurs when $d\Delta/d\bar{P}_1(t_{eq}) = 0$ in the interval $0 < \bar{P}_1(t_{eq}) \leqslant 1$ with the value $1 - 1/\gamma_1 \leqslant \Delta_{max} < \Delta_1 \leqslant 1$, where unity is approached by Δ_1 as $\bar{P}_1(t_{eq}) \to 0$. Expressions [A.9]

and [A.11] are valid whenever $V' \gg 1$, $\gamma_1 \to 1$ or $\alpha = \beta$ with $\bar{T}_2(0) = 1$, as separate cases or in combination, and then $\bar{P}(\infty) = \bar{P}_1(t_{eq})$ if $\bar{T}(\infty) = 1$.

It is of interest to examine the mass defect (as defined by [A.8]), and the pressure ratio

$$P_r \equiv \frac{\bar{P}_1(t_{eq})}{\bar{P}(\infty)} \qquad [A.12]$$

using the numerical solution of [37] when $\alpha \neq \beta$, $\gamma_1 \neq 1$ and V' is finite, to determine if significant departures from the special cases can exist. For such general cases, if $\bar{T}(\infty)$ is included, nine independent parameters affect the results for Δ and P_r. The detailed comparisons of that study are included in Chenoweth & Paolucci (1990a). The behavior resulting in $P_r \neq 1$ is analogous in some respects to that found for ideal gas mixing involving different temperatures and different internal molecular structure (see Chenoweth & Paolucci 1989).